QUENCHING-RESOLVED EMISSION ANISOTROPY STUDIES WITH SINGLE AND MULTITRYPTOPHAN-CONTAINING PROTEINS

MAURICE EFTINK
Department of Chemistry, University of Mississippi, University, Mississippi 38677

ABSTRACT Measurements of the anisotropy of protein fluorescence as a function of an added collisional quencher, such as acrylamide, are used to construct Perrin plots. For single tryptophan containing proteins, such plots yield an apparent rotational correlation time for the depolarization process, which, in most cases, is approximately the value expected for Brownian rotation of the entire protein. Apparent limiting fluorescence anisotropy values, which range from 0.20 to 0.32 for the proteins studied, are also obtained from the Perrin plots. The lower values for the limiting anisotropy found for some proteins are interpreted as indicating the existence of relatively rapid, limited (within a cone of angle 0°–30°) motion of the trytophan side chains that is independent of the overall rotation of the protein. Examples of the use of this fluorescence technique to study protein conformational changes are presented, including the monomer ⟷ dimer equilibrium of β-lactoglobulin, the monomer ⟷ tetramer equilibrium of melittin, the N ⟷ F transition of human serum albumin, and the induced change in the conformation of cod parvalbumin caused by the removal of Ca^{+2}. Because multitryptophan-containing proteins have certain tryptophans that are accessible to solute quencher and others that are inaccessible, this method can be used to determine the steady state anisotropy of each class of tryptophan residues.

INTRODUCTION

Studies of the anisotropy of the fluorescence of tryptophanyl residues in proteins can provide valuable information concerning the dynamics of these macromolecular structures. For relatively small globular proteins the overall Brownian rotation of the protein can lead to a significant degree of depolarization of the tryptophanyl fluorescence. In addition, rapid internal rotational modes of the residue side chains and interresidue resonance energy transfer can also result in a loss of emission anisotropy (1).

Experimental observation of these effects can be made via time-resolved emission anisotropy decay studies. Several anisotropy decay studies have been performed on conjugates between extrinsic fluorescent probes and proteins (e.g., immunoglobulins, [2–4] and muscle proteins, [5,6]). Technical developments in recent years have enabled anisotropy decay studies to be made on the intrinsic tryptophanyl fluorescence of proteins as well (7–9). In these anisotropy decay studies, a range of fluorophore rotational correlation times has been observed. In some cases, the rotational correlation times correspond to depolarization due to global rotation of the macromolecule; in other cases, the data indicate the existence of internal or segmental motion of the fluorescing group.

Similar information concerning the motion of tryptophanyl residues (or other extrinsic probes) in proteins can be obtained from steady state measurements of emission anisotropy as a function of T/η (10–15). This approach is commonly used, but different results are often obtained depending on whether the experiments are performed by varying temperature or the bulk viscosity (see discussion in Concluding Remarks).

Another steady state approach, used first by Teale and Badley (16), involves the measurement of the emission anisotropy of a protein as a function of added collisional quencher. By lowering the fluorescence lifetime of the fluorophore in this manner and by measuring the resulting emission anisotropy increase one can determine the rotational correlation time of the fluorescent residue (heterogeneously emitting systems can be more complicated; see Theory section below). In recent years Lakowicz, Weber, and co-workers (17, 18) have used this approach in connection with their oxygen quenching studies with proteins. We offer the name "quenching-resolved emission anisotropy" (QREA)[1] for such experiments.[2]

[1] *Abbreviations used in this paper:* ACTH, adrenocorticotropic hormone; HSA, human serum albumin; LADH, horse liver alcohol dehydrogenase; QREA, quenching resolved emission anisotropy; λ_{ex}, excitation wavelength; λ_{em}, emission wavelength.

[2] The name lifetime-resolve fluorescence anisotropy has been previously used for such experiments (17), but, as pointed out by a reviewer, quenching resolved emission anisotropy is a more general description of the technique. For example, for the case of a protein possessing two types of Trp residues, one accessible and one inaccessible to a collisional quencher, it is possible that the average fluorescence lifetime of the protein may not decrease significantly upon adding quencher (i.e., if the lifetime of the inacessible residue is about the same as or longer than that of the accessible residue). In such a case, the meaning of "lifetime-resolved" becomes complicated. Also selective static quenching may potentially find use in the resolution of the fluorescence anisotropy of multi-Trp proteins.

When oxygen is used as the quenching probe, as in the above-mentioned works, one can, to a first approximation, assume that all fluorescing tryptophanyl residues in a multitryptophan-containing protein will be quenched to the same degree. This is based on the findings of a rather narrow range of rate constants for the oxygen quenching of a variety of proteins (19). (However, see reference 20 for a recent study in which the range of rate constants has been extended and selective quenching by oxygen has been observed.) On the one hand, this property of oxygen quenching simplifies matters by allowing a multitryptophan-containing protein to be treated essentially as a homogeneous system. On the other hand, a degree of selectivity in quenching would be desirable for QREA studies with certain proteins to enable one to focus on the rotational behavior of different classes of tryptophanyl residues.

Acrylamide and iodide are efficient and convenient fluorescence quenchers that have been found to preferentially quench the more solvent-exposed tryptophanyl residues in multitryptophan proteins (21, 22) and should, therefore, be excellent candidates for use in QREA experiments. For example, both of these quenchers have been found to selectively quench the fluorescence of the surface Trp residue (Trp 15) of horse liver alcohol dehydrogenase (LADH) to a much greater extent than the internal Trp residue (Trp 314) (9,23,24).

In this paper we will present QREA studies with a number of proteins using these polar quenchers (primarily acrylamide). Studies with a variety of single-Trp–containing proteins will first be presented to illustrate the way in which information can be obtained about global and internal rotational motions of the proteins. We will also demonstrate the use of QREA to monitor ligand-induced conformational changes in proteins and protein-protein aggregation reactions. Finally, we will combine the selective quenching of polar quenchers with the QREA technique to try to resolve the dynamic characteristics of individual Trp residues in multi-Trp proteins (e.g., LADH).

THEORY

Rigidly Attached Fluorophore

The decrease in the emission anisotropy, r, from its limiting value, r_o (i.e., in absence of motion), due to isotropic rotation of a fluorophore is given by the following version of the Perrin equation

$$1/r = 1/r_o + \tau/r_o\phi \tag{1}$$

where ϕ is the rotational correlation time describing the depolarization process. Isotropic depolarization would correspond to a fluorophore being rigidly attached to a spherical macromolecule.

If the fluorescence lifetime, τ, can be decreased by the addition of a collisional quencher, the rotational correlation time and limiting anisotropy can be directly obtained from a plot of $1/r$ vs. τ (16). (This assumes that τ and ϕ are of the same order of magnitude.) The drop in τ with added quencher, Q, is given by the Stern-Volmer relationship.

$$\tau = \frac{\tau_o}{1 + K_{sv}[Q]} \tag{2}$$

where τ_o is the lifetime in the absence of quencher and K_{sv} is the Stern-Volmer collisional quenching constant (which is equal to $k_q\tau_o$ where k_q is the biomolecular rate constant for the quenching reaction).

The ϕ value obtained in this manner can be compared with the rotational correlation time, ϕ_h, for a hydrated sphere that can be calculated from the following equation:

$$\phi_h = \frac{M(\bar{v} + h)\eta}{kT} \tag{3}$$

where M is the molecular weight, $\bar{v}$ is the partial specific volume, h is the degree of hydration of the sphere, and η is the viscosity of the medium. Because one can assume values of $\bar{v} = 0.73$ cm^3/g and $h = 0.3$ cm^3/g for most proteins (25), the rotational correlation time for overall, global rotation of a globular protein having a given molecular weight can readily be estimated.

In reality, however, globular proteins may not behave as rigid spheres; the rotation of the protein may be nonisotropic due to its structural asymmetry, or internal depolarizing motions of the Trp side chains may take place (see Results and Discussion below). For a protein having the shape of an ellipsoid and having fluorophores rigidly attached and randomly distributed on its surface (i.e., a multi-Trp protein), the apparent ϕ obtained from analysis of fluorescence anisotropy data with Eq. 1 will be the mean harmonic rotational correlation time for rotation about the major and minor axes of the ellipsoid. This ϕ(app) will be larger than the ϕ_h calculated from Eq. 3 for a spherical protein of equivalent molecular weight. For an asymmetric protein containing a fluorophore rigidly attached at a fixed angle with respect to the major axis of the ellipsoid (i.e., a single-Trp protein), the anisotropy decay will be a multi-exponential process (in most cases ony two decay rates are expected to be resolvable [26,27]). In such a case, a plot of $1/r$ vs. τ would be nonlinear. For relatively small axial ratios, however, the deviation from linearity would be expected to be small, and the apparent ϕ obtained would depend not only on the size and shape (axial ratio) of the macromolecule, but also on the angle between the major axis of the ellipsoid and the absorption (and emission) transition moment of the fluorophore (6, 10, 16). Depending on this angle, the ϕ(app) for depolarization of the emission may be greater than or less than the mean harmonic rotational correlation time for global rotation of the macromolecule.

Internal Motion of Fluorophores

If the fluorophores attached to a spherical macromolecule enjoy rapid, restricted motion, such as that expected for the rotation of a side chain about its covalent link, the Perrin equation describing the emission anisotropy for such a system takes on the following form (2, 12, 28):

$$r = r_o\left(\frac{F_1}{1 + \tau/\phi_1} + \frac{F_2}{1 + \tau/\phi_2}\right) \tag{4}$$

where ϕ_1 and ϕ_2 are the rotational correlation times for global and internal rotation of the fluorophore and F_1 and F_2 are weighting factors for the respective depolarizing processes. (Eq. 4 assumes that the internal motion is much faster than the overall rotation of the macromolecule [i.e., $\phi_1 >> \phi_2$]. As pointed out by Lipari and Szabo [29], if this condition does not hold, the effective rotational correlation time for internal motion will contain a contribution from both the overall and internal rotational correlation times. Because ϕ_2 is not determined in our experiments and because the condition of $\phi_1 >> \phi_2$ is probably realized in most cases where internal motion does occur, we feel that Eq. 4 is adequate for our purposes.)

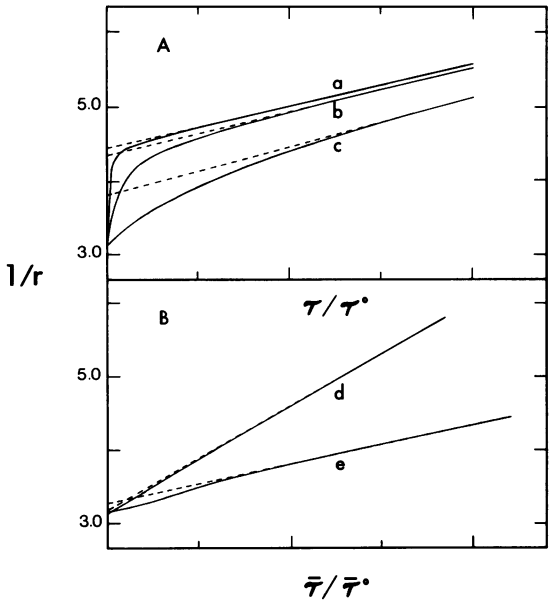

FIGURE 1 (*A*) Simulated QREA Perrin plots for a fluorophore that is depolarized by both overall rotation of the macromolecule to which it is attached (characterized by ϕ_1 = 20 ns) and by independent segmental motion of the fluorophore (characterized by ϕ_2 = 0.01 ns in *a*; ϕ_2 = 0.1 ns in *b*; and 1.0 ns in *c*). In each case τ_o =5 ns, r_o = 0.32, F_1 = 0.7 and F_2 = 0.3 (see Eq. 4). This value of F_2 corresponds to θ = 26.5° in Eq. 5. The apparent ϕ, r_o, and θ values obtained from dashed lines drawn above are given in Table I. (*B*) Simulated QREA plots for a heterogeneously emitting fluorophore having a single rotational correlation time (see Theory Section Multicomponent Emission From Single-Trp Protein in text). It is assumed that r_o = 0.32, ϕ = 5 ns, τ_1^o = 5 ns, τ_2^o = 0.5 ns, and, for curve *d*, F_1 = 0.909, F_2 = 0.091 (corresponds to $\alpha_1 = \alpha_2$ = 0.5); for curve *e*, $F_1 = F_2$ = 0.5 (corresponds to α_1 = 0.09 and α_2 = 0.91).

In Fig. 1 *A* we present simulations of QREA experiments for systems described by the above equation. The resulting plots of $1/r$ vs. τ will be in general nonlinear, but will appear roughly linear over the large values of τ. In Table I we present values of ϕ(app) and r_o(app) that one would graphically determine from the simulated data from the slope and intercept of the dashed lines. If the ϕ_2/ϕ_1 ratio is very small (internal motion if very rapid), the resulting plot will appear linear and the determined ϕ(app) will be only slightly $<\phi^1$. The r_o(app), on the other hand, will appear to be much lower than the true value. As the ϕ_2/ϕ_1 ratio increases (i.e., as the internal motion becomes slower), the $1/r$ vs. τ plots appear more curved and the ϕ(app) values become smaller than ϕ_1. Thus, if internal motion exists, the ϕ(app) values are a lower estimate of the rotational correlation time for global rotation of the macromolecule. The r_o(app) values remain less than the true r_o, but approach the latter value as ϕ_2/ϕ_1 increases.

TABLE I
APPARENT ROTATIONAL CORRELATION TIMES AND LIMITING ANISOTROPIES FROM SIMULATED QREA PERRIN PLOTS FOR A SYSTEM HAVING SEGMENTAL MOTION OF A BOUND FLUOROPHORE*

Curves in fig. 1	ϕ_2	ϕ(app)	r_0(app)	θ(app)
	ns	*ns*		*deg*
a	0.01	19.1	0.226	25.5
b	0.1	17.6	0.232	24.4
c	1.0	13.4	0.268	18.0

*From data simulations in Fig. 1; ϕ_2 and r_0 are assumed to be 20 ns and 0.32, respectively. F_1 and F_2 (see Eq. 4) are assumed to be 0.3 and 0.7, respectively. The true value of θ is 26.5°.

The r_o(app) values can provide additional information concerning the nature of the internal motion in terms of the angular displacement of such restricted motion as given by the following relationship (10, 28):

$$r_o(\text{app})/r_o \approx F_2 = (3\cos^2\theta - 1)/2 \qquad (5)$$

where θ is the average angle over which the Trp residue (or other fluorophore) can rotate independently. For example, in curve *a* of Fig. 1 *A*, the rapid independent motion of the fluorophore can be described as occurring within a cone of average angle of 25.5°. Thus dynamic information can be obtained in QREA experiments from both the ϕ(app) and r_o(app) values.

Multicomponent Emission from Single Trp Proteins

It has become apparent in recent years that the fluorescence decay of many single Trp containing proteins, and even tryptophan itself, must be characterized by at least a double exponential (30, 31). The basis for this lifetime heterogeneity is presently a matter of great concern and may involve either ground state or excited state heterogeneity. The question we would like to address is what effect this emission heterogeneity for single-Trp proteins will have on data obtained in QREA experiments.

Consider the case in which the fluorescence decay, $S(t)$, of a Trp residue (or other fluorophore) of a protein is characterized by two lifetimes (τ_1 and τ_2), as follows

$$S(t) = \alpha_1 e^{-t/\tau_1} + \alpha_2 e^{-t/\tau_2}. \qquad (6)$$

Let us assume that, although the fluorescence decay is nonexponential for some reason, the fluorescence anisotropy decay, $r(t)$, is exponential, with depolarization described by a single rotational correlation time, ϕ, corresponding to the global rotation of the protein, $r(t) = r_o e^{-t/\phi}$. From this the steady state anisotropy is given as

$$r = \frac{\int_0^\infty r_0 e^{-t/\phi}(\alpha_1 e^{-t/\tau_1} + \alpha_2 e^{-t/\tau_2})\,dt}{\int_0^\infty (\alpha_1 e^{-t/\tau_1} + \alpha_2 e^{-t/\tau_2})\,dt} \qquad (7)$$

which upon integration yields

$$r = \frac{r_o f_1}{1 + \tau_1/\phi} + \frac{r_o f_2}{1 + \tau_2/\phi} \qquad (8)$$

where $f_i = \alpha_i\tau_i/\Sigma\alpha_i\tau_i$ and α_i are the preexponential terms in Eq. 6.

In Fig. 1 *B* we present simulated QREA experiments for the above type of system for cases in which τ_1 = 5.0 ns, τ_2 = 0.5 ns and ϕ = 5.0 ns. (Note that in this plot $\bar{\tau}$ is the weighted average fluorescence lifetime, which is equal to $\Sigma f_i\tau_i$.) The two curves are for different α_1/α_2, the ratio of the long to the short lifetime component. The ϕ(app) determined from the dashed lines drawn through these curves are 5.66 ns (curve *d*) and 7.52 ns (curve *e*). The r_o(app) for curves *d* and *e* are 0.312 and 0.305, respectively. Thus, lifetime heterogeneity for this single-Trp protein model has the effect of slightly increasing the apparent ϕ and slightly decreasing the apparent r_o.

It is interesting that this multi-component lifetime effect leads to a slight increase in ϕ(app), whereas the existence of internal motion leads to a decrease in ϕ(app). In a real protein both of these effects are expected to be important. Depending on the relative significance of each of these effects, the apparent ϕ determined from QREA experiments can be

expected to be either larger than or smaller than the true ϕ for global rotation of the macromolecule. If the effects roughly cancel (or if neither is significant), ϕ(app) will be a good estimate of ϕ_h.

Multitryptophan-containing Proteins

The steady state emission anisotropy of multi-Trp proteins is equal to the weighted sum of each residue as follows

$$r = \Sigma f_i r_i \tag{9}$$

where r_i and f_i are the anisotropy and fractional steady state emission intensity of each residue (note that f_i may be excitation and emission-wavelength dependent).

The following three possible cases come to mind for QREA studies with such multi-Trp proteins:

(*a*) k_{qi} and ϕ_i are approximately the same for all fluorophores; τ_i are different. For this case all the fluorophores would be equally exposed to the quencher, would depolarize with equal correlation time (the simplest situation being that in which there is no internal motion of the residues and all $\phi_i = \phi_h$), but would have different lifetimes. This corresponds to the section above for multicomponent emission from a protein. The resultant plots of $1/r$ vs. $\bar{\tau}$ (where $\bar{\tau} = \Sigma f_i \tau_i$) would appear as those in Fig. 1 *B*. The resultant ϕ(app) would be slightly larger than or equal to ϕ_h, and r_o(app) would be slightly $< r_o$. This case may be realized experimentally in studies with a relatively nonselective quencher, such as oxygen (17).

(*b*) k_{qi} and τ_i are approximately the same for all fluorophores; ϕ_i are different. Here the K_{svi} ($= k_{qi}\tau_i^o$) for each residue is the same, but there is a difference in the rotational correlation times of the residues, presumably due to the existence of a different degree of independent motion of the various residues. This is analogous to the case presented in Internal Motion of Fluorphores above and the resultant plot of $1/r$ vs. $\bar{\tau}$ would appear similar to those in Fig. 1 *A*. The existence of rapidly depolarizing residues (i.e., small ϕ_i) would lead to a decrease in r_o(app). The slope drawn through the data at high $\bar{\tau}$ would yield a ϕ(app) estimate that is less than or equal to the largest ϕ_i.

Again, this case may be observed in studies with a relatively nonselective quencher such as oxygen. Lakowicz and Weber (17) have presented simulations for such a case. The basic difference between this and the preceeding case is in whether there is a greater variation in the fluorescence lifetime of different Trp residues in a protein or in the rotational correlation time of the residues. The range of fluorescence lifetimes of Trp residues in proteins appears to be 0.5–10 ns. The values of ϕ_i may vary over an equally wide range as demonstrated by the work of Munro et al. (8).

(*c*) τ_i and ϕ_i are approximately the same for all fluorophores; k_{qi} widely different (selective quenching). In this case the addition of quencher selectively quenches the fluorescence of the accessible class of Trp residues and the anisotropy of the remaining fluorescence increasingly reflects the anisotropy of the inaccessible class of Trp residues. If, for simplicity, one considers each fluorescing residue to be described by Eq. 1 (i.e., single τ and ϕ for each residue and all having the same r_o), the anisotropy of the total emission is

$$r = r_o \sum_{i=1}^{n} \frac{f_i}{1 + \tau_i/\phi_i} \tag{10}$$

where $f_i = F_i/F$ is the fractional steady state fluorescence intensity of each residue, F_i is the fluorescence intensity of residue *i*, and $F = \Sigma F_i$ is the total fluorescence intensity. If there are only two classes of Trp residues, one (residue No. 1, $f_1, \tau_1, \phi_1, k_{q1}$) that is accessible to quencher and the other (residue No. 2, $f_2, \tau_2, \phi_2, k_{q2}$) inaccessible to quencher, the above equation simplifies to Eq. 8. Furthermore, τ_2 will be independent of the concentration of quencher ($\tau_2 = \tau_2^o$ in Eq. 2, since k_{q2} is assumed to be zero) and τ_1 will decrease with added quencher according to $\tau_1^o/(1 + k_{q1}\tau_1^o[Q])$. Simulated QREA Perrin plots for such a system are shown in Fig. 2 *A*. In this figure we have plotted $1/r$ vs. F rather than $\bar{\tau}$; the reason

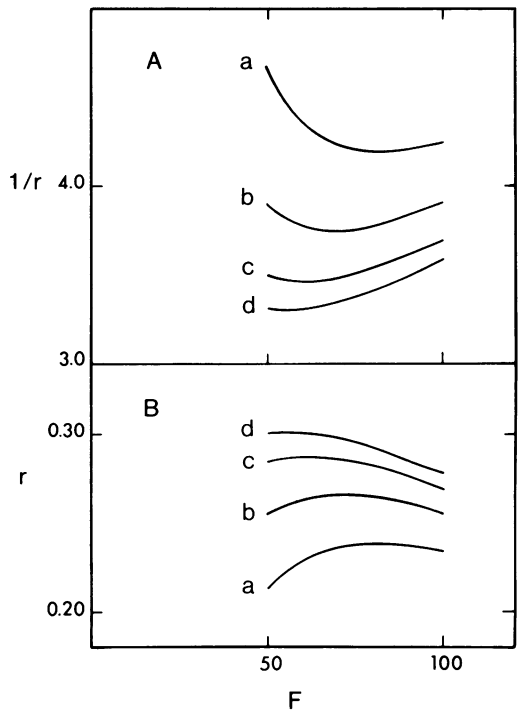

FIGURE 2 Simulated QREA Perrin plot (*A*) and direct plot of r vs. F (*B*) for a system in which selective quenching is obtained (Theory section Multitryptophan-containing Proteins in text). It is assumed that residue No. 1 is quenched and that residue No. 2 is not, and that $\tau_1^o = 5$ ns, $\phi_1 = 20$ ns ($\tau_1^o/\phi_1^o = 1/4$), and $r_o = 0.32$ for both residues. The various curves shown correspond to the selection of the ratio of τ_2^o/ϕ_2 as 1/2 (*a*), 1/4 (*b*), 1/8 (*c*), and 1/16 (*d*).

for using F instead of $\bar{\tau}$ as the abcissa will become clear below. Also shown is a direct plot of r vs. F in Fig. 2 *B*.

The simulations show that when selective quenching occurs the Perrin plot can be curved. One cannot obtain meaningful ϕ(app) and r_o(app) from forced-fit lines drawn through such plots. Instead, however, one can determine the anisotropy of each class of residue in the following way. At $[Q] = 0$ (at F_o), r is the weighted average, equal to $f_1 r_2 + f_2 r_2$. At $[Q] = \infty$, the remaining fluorescence intensity and anisotropy are F_2 and r_2, that of the inaccessible class of residues. The ratio F_2/F_o is f_2, the fractional intensity of the inaccessible residues at $[Q] = 0$, from which f_1 can be obtained as $1\text{-}f_2$. Knowing f_1, f_2, and r_2, one can calculate r_1 from the value of r in the absence of quencher.

Note that since the observed emission anisotropy can either increase or decrease on the addition of a selective quencher to a multi-Trp–containing protein, that one must be judicious about using such QREA Perrin plots as proof that a particular quencher is a collisional quencher.

Effect of Static Quenching on QREA Perrin Plots

Because the fluorescence intensity of a protein sample is usually proportional to its fluorescence lifetime, it will be more practical in most laboratories to construct QREA Perrin plots of $1/r$ vs. F instead of τ. For studies with multi-Trp proteins using selective quenchers, it is desirable to make fluorescence intensity measurements instead of lifetime measurements, since the intensity values can be used to determine the fractional contribution of various classes of Trp residues (f_i values), whereas average lifetime values cannot.

The substitution of intensity for lifetime measurements in QREA experiments is valid if the added quencher is a collisional quencher. (Note

that in selective quenching studies with multi-Trp proteins, the quencher can be a static quencher.) However, a certain degree of static quenching is often observed in studies with proteins. For example, with acrylamide as quencher in studies with a number of single Trp containing proteins, the static quenching component is often found to be ~10% of the collisional component (21). If in QREA experiments some of the quenching does occur statically, this can lead to a slight overestimate of ϕ(app) and an underestimate of r_o(app) if the static quenching is neglected. Simulations have been presented elsewhere to illustrate this point (32). One can correct for static quenching by plotting $F \exp(V[Q])$ in QREA Perrin plots, instead of F (where V is the static quenching constant).

EXPERIMENTAL

Materials

Rabbit muscle aldolase, glucagon, β-lactoglobulin, horse liver alcohol dehydrogenase (lyophilized), hen lysozyme, bee venom melittin, human serum albumin, porcine phospholiphase A_2, monellin from *Dioscoreophyllum comminsii* and nuclease from *Staphylococcus aureus* were all obtained from Sigma Chemical Co. St. Louis, MO. Rabbit myelin basic protein and crystallized horse liver alcohol dehydrogenase were obtained from Calbiochem-Behring Corp., American Hoechst Corp., San Diego, CA.

The phospholiphase A_2 was passed through a Sephadex G-25 column before use. Glucagon was dissolved in 0.1 M NaCl, pH 3.0 solution. Serum albumin was defatted according to the procedure of Chen (33), and was then passed through a Sephadex G-100 column to separate the monomer from higher aggregates. The lyophilized alcohol dehydrogenase was purified by a heat treatment described elsewhere (24). The alcohol dehydrogenase treated in this manner gave identical results as the crystallized preparation from Calbiochem-Behring Corp. As described elsewhere (24), these LADH preparations are generally found to be > 90% active. Lysozyme was chromatographed on CM-sephadex at pH 10.0 (0.05 sodium borate, 0.15 M NaCl buffer) before use.

A purified sample of ribonuclease T_1 from *Aspergillus oryzae* was a generous gift from Dr. F. Walz, Kent State University. fd bacteriophage was a generous gift from Dr. R. Webster, Duke University. Cod parvalbumin was prepared (single band in SDS-gel electrophoresis) following the procedure of Horrocks and Collier (34). Ca^{+2} was removed from this protein as described by Blum et al. (35).

Unless stated otherwise, all proteins were dissolved or dialyzed into a 0.033 M phosphate buffer, pH 7.0, for the fluorescence studies. Solutions were made using distilled, deionized water and were usually passed through a millipore filter before the fluorescence measurements were taken. Acrylamide was recrystallized from ethyl acetate and an 8 M stock solution was prepared for the quenching studies. A 5 M stock solution of KI was prepared, with ~10^{-4} M $Na_2S_2O_3$ added to prevent oxidation.

Methods

Fluorescence anisotropy measurements were made using a Perkin-Elmer MPF-44A spectrophotofluorometer. A thermo-regulated cell holder was used and excitation and emission bandwidths of 5 and 10 nm, respectively, were used on all occasions. An excitation wavelength of 300 nm was used for all QREA experiments; the emission wavelength used was usually 345 nm. This wavelength is > 10 nm removed from the center of the Raman scattering peak. On some occasions, particularly with the blue emitting proteins RNAse T_1 and parvalbumin, an emission wavelength of 320 nm was used.

HNB Polaroid polarizers (Polaroid Corp., Cambridge, MA) were used for most studies. The steady state anisotropy, r, of the fluorescence signal was measured as

$$r = \frac{F_{VV} - F_{VH}g}{F_{VV} + 2F_{VH}g} \qquad (11)$$

where F_{VV} and F_{VH} are the vertical (parallel) and horizontal (perpendicular) components of the emitted light when excited with vertically polarized light. The factor g, which serves to correct for emission monochrometer polarization effects, is equal to the ratio F_{HH}/F_{HV}, where F_{HH} and F_{HV} are the horizontal and vertical components of emission from horizontally polarized exciting light. The value of g with our instrument ranges from 1.0 at 370 nm to 1.15 at 320 nm. The F_{VV} and F_{VH} values in Eq. 11 were corrected for background fluorescence and the transmission of scattered excitation light by substracting the signal observed from control buffer solutions that contained no protein (36). Usually this correction is negligible, but upon quenching the fluorescence signal, the background correction can become important. Also, since all protein solutions had negligible turbidity, depolarization due to scattering of the polarized excitation and emission photons was judged to be insignificant (37). The precision of r measurements was approximately ±0.005.

The HNB polarizers used allow a slight passage (or leakage) of orthogonal light. This leakage is only ~1–2% at the wavelength studied (leakage measured by the F_{VH}/F_{VV} ratio of scattered light from a glycogen-containing solution). The existence of such leakage leads to an artificial lowering of the observed anisotropy from its true value. With the HNB polarizers this discrepancy is very small (only a few percent of most measured r values) and can be neglected. Some of our studies were done with Polacoat polarizers (Perkin-Elmer Corp., Norwalk, CT). The orthogonal light leakage of these polarizers is quite high (~8%), and the apparent r values measured with these polarizers are significantly lower than the values measured with HNB polarizers. For example, the apparent r of *N*-acetyl-L-tryptophanamide dissolved in glycerol at 25° are 0.165 and 0.195, respectively, using Polacoat and HNB polarizers. For the few studies in which Polacoat polarizers were used, the apparent r values were corrected for the effect of polarizer light leakage using the equations given in Perkin-Elmer technical bulletin FL-74.

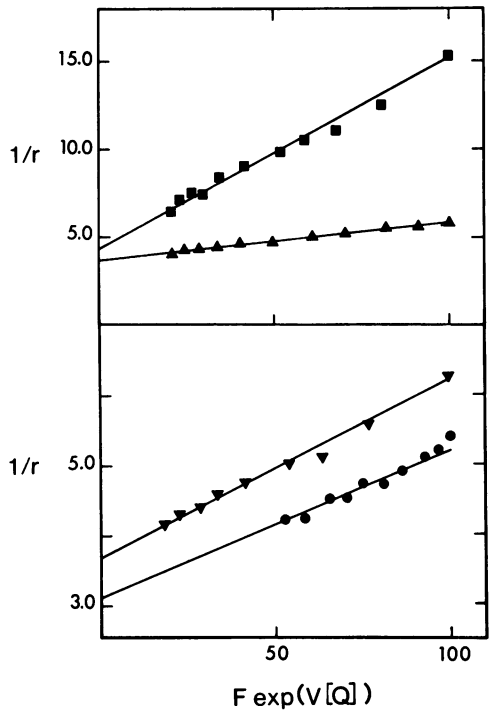

FIGURE 3 QREA Perrin plots for the acrylamide quenching of glucagon (■), nuclease (▲), monellin (▼), and ribonuclease T_1 (●). Excitation at 300 nm; emission at 345 nm for glucagon, nuclease, and monellin and 320 nm for ribonuclease T_1. Conditions given in Table II. To determine ϕ(app), as defined by Eq. 1, the slope of the plot was determined by setting F_o equal to the fluorescence lifetime of the protein.

For QREA experiments, F_{VH} and F_{VV} measurements on a protein containing solution were made with the addition of aliquots of stock quencher solutions. All corrections for dilution of the solution and internal screening effects were made as necessary ([21] $\epsilon_{300} = 0.11\ M^{-1}\ cm^{-1}$ for acrylamide). All protein solutions had an initial optical density of 0.03 or higher at 300 nm. The slope and intercept of QREA Perrin plots were obtained by linear regression (i.e., the plots were assumed to be straight lines; no attempt was made to analyze for curvature as predicted by the simulations in Fig. 1 and Theory sections, Internal Motion of Fluorophores and Multicomponent Emission from Single Trp Proteins).

Fluorescence lifetimes were measured with a SLM 4800 phase fluorometer (SLM Instruments, Inc., Urbana, IL) or were obtained from the literature.

RESULTS AND DISCUSSION

Studies with Single Tryptophan Containing Proteins

QREA Perrin plots obtained for a number of single-Trp–containing proteins, using acrylamide as quencher, are shown in Fig. 3. The apparent r_0 and ϕ obtained for these and other proteins by analysis of data with Eq. 2 are given in Table II. In these Perrin plots, $1/r$ is plotted vs. the steady state fluorescence intensity, F, and, in those cases

TABLE II

QUENCHING RESOLVED EMISSION ANISOTROPY AND ACRYLAMIDE QUENCHING DATA FOR SINGLE AND MULTI-TRP CONTAINING PROTEINS AND POLYPEPTIDES*

Single-trp proteins (molecular weight)	Acrylamide quenching data				QREA data			
	τ_0	$k_q \times 10^{-9} M^{-1}s^{-1}$	V	r	ϕ_h	ϕ(app)	r_0(app)	θ
	ns		M^{-1}		*ns*	*ns*		degrees
Ribonuclease T_1‡ 11,000	3.6§	0.20	—	0.185	4.1	5.2	0.320	0°
Parvalbumin 12,000	3.4‖	0.24	—	0.150	4.4	3.7	0.290	12°
Parvalbumin, $-Ca^{+2}$ 12,000	3.5‖	2.5	—	0.118	4.4	4.9	0.205	28°
HSA, pH 7 (N form) 69,000	6.0¶	0.76	0.8	0.224	25.6	31.0	0.265	18°
HSA, pH 3.5 (F form) 69,000	3.3¶	1.0	0.4	0.230	25.6	10.9	0.298	9°
Nuclease ¶¶ 20,000	5.0¶	0.80	0.2	0.175	7.4	9.1	0.265	18°
Monellin 10,700	2.6¶	2.0	0.2	0.160	4.1	3.7	0.270	17°
Phospholipase A_2¶¶ 13,900	3.2§	2.2	0.1	0.165	5.2	5.1	0.270	17°
Myelin basic protein 18,000	2.8**	2.2	—‖‖	0.137	6.7	2.8	0.280	15°
Melittin, monomer 2,800	3.0‖	2.9	1.0	0.092	1.0	1.5	0.270	17°
Melittin, tetramer 11,200	2.3‖	1.5	0.5	0.140	4.2	2.5	0.265	18°
Glucagon 3,500	2.8¶	3.0	0.7	0.065	1.3	1.1	0.220	26°
ACTH 4,500	3.1¶	3.2	1.0	0.081	1.7	1.7	0.217	27°
Multi-Trp Proteins								
β-lactoglobulin, monomer 18,000	2.0‖	0.55	—	0.244	6.7	8.4	0.305	
β-lactoglobulin, dimer 36,000	1.9‖	0.50	—	0.275	13.4	15.4	0.310	
Lysozyme 14,000								
accessible Trp	2.0‡‡	2.0	—	0.170	5.3		(see text)	
inaccessible Trp	0.5‡‡	0	—	0.265	5.3		(see text)	
LADH 80,000								
accessible Trp (Trp 15)	7.0§§	1.3	—	0.210	29.6		(see text)	
inaccessible Trp (Trp 314)	4.0§§	<0.05	—	0.263	29.6		(see text)	

*Temperature, 25°C. Fluorescence quenching data (F_0/F vs $[Q]$ were analyzed with Eq. 3 of Eftink and Ghiron (21). QREA data ($1/r$ vs F) were analyzed with Eq. 1. ϕ_h and θ values were calculated using Eqs. 2 and 5, respectively (with r_0 taken as 0.31). The error limits in the ϕ(app) and r_0(app) values are approximately ±10% and ±3%, respectively (neglecting error in the τ_0 values) in most cases. For those proteins in which k_q is low, (i.e., ribonuclease T_1 and parvalbumin), the error limits on ϕ(app) and r_0(app) are approximately twice as large.

‡The following proteins were used with the buffers indicated. Ribonuclease T_1, parvalbumin, HSA (N form), monellin, phospholipase A_2, ACTH, lysozyme, and LADH, phosphate buffer, 0.033 M, pH 7; HSA (F form), formate buffer, 0.1 M, pH 3.0; nuclease, Tris buffer, 0.01 M, 0.01 M $CaCl_2$, pH 7; myelin basic protein, Tris buffer, 0.01 M, pH 7; melittin (monomer), phosphate buffer, 0.02 M, pH 7; melittin (tetramer), phosphate buffer, 0.5 M, pH 7; glucagon, 0.1 M NaCl, pH 3; β-lactoglobulin (monomer), formate buffer, 0.03 M, pH 2.4; β-lactoglobulin (dimer), acetate buffer, 0.1 M, pH 4.5.

§Determined with a cross-correlation phase fluorometer of Spencer and Weber (57) operating at 18 MHz from the phase lag.

‖Determined with a SLM phase correlation fluorometer operating at 30 MHz; τ_0 value is the average of that from the phase lag and degree of modulation.

¶From reference (21). The lifetimes are single exponential fits to fluorescence decay kinetics.

**From reference (8).

‡‡From reference (50).

§§From references (9) and (20), adjusted to 25°C.

‖‖Stern-Volmer plot is slightly downward curving due, most likely to an impurity in the sample.

¶¶QREA data obtained using Polacoat polarizers (Perkin-Elmer Corp.); anisotropy values corrected as described in Materials and Methods section.

where the acrylamide static quenching constant, V, is significant (see Table II and reference 21) $1/r$ is plotted vs. $F \exp(V[Q])$.

The anisotropy measurements were made with an excitation wavelength of 300 nm, in all cases. The fluorescence anisotropy of indole derivatives and proteins is quite dependent on excitation wavelength, as demonstrated by Weber (38). A minimum in the excitation anisotropy spectrum of such compounds is generally seen at ~290 nm, corresponding to excitation into the ^1L_b band of indole. With excitation at ~300 nm and above, a maximum in the excitation anisotropy spectrum is seen, due to selective excitation into the ^1L_a band (38, 39). Fig. 4 illustrates the excitation anisotropy spectrum of three selected proteins, ribonuclease T_1, monellin, and gluagon (representing cases of Trp residues of various degree of solvent exposure). In each case, the anisotropy is low, between 270–290 nm, and increases to a plateau between 300 and 305 nm. For our studies, an excitation wavelength of 300 nm was selected as a trade-off between fluorescence intensity and the desire to excite into the plateau region. Also, by exciting into the red edge of the absorption spectrum, homo-transfer between Trp residues (in multi-Trp proteins) is eliminated as a possible depolarizing process (40).

The emision wavelength monitored for most of our studies was 345 nm (to avoid the Raman band), except for the very blue emitting proteins, for which 320 nm was used. This raises the question as to whether the emission anisotropy of Trp residues in proteins varies with emission wavelength. Also shown in Fig. 4 is the emission wavelength dependence of r for selected proteins. As can be seen, for some proteins such as monellin, r decreases with increasing wavelength. For glucagon, r also decreases with wavelength, but not as rapidly. Ribonuclease T_1 and

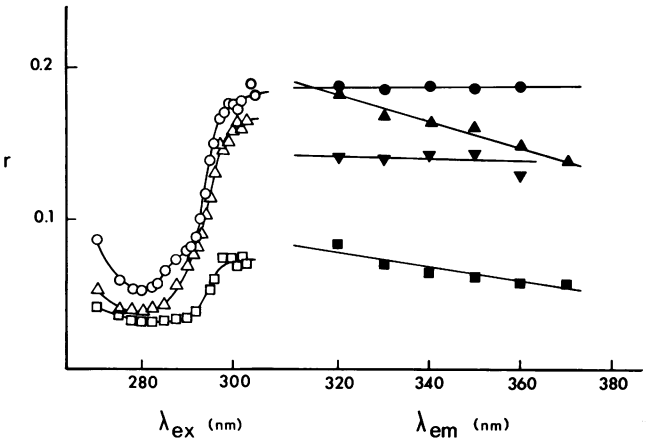

FIGURE 4 (*Left*) Excitation anisotropy spectra of glucagon (□), monellin (△) and ribonuclease T_1 (○). Emission monitored at 345 nm for glucagon and monellin and 320 nm for ribonuclease T_1. Conditions given in Table II. (*Right*) Emission wavelength dependence of the anisotropy of glucagon (■), monellin (▲), parvalbumin (▼), and ribonuclease T_1 (●). Excitation at 300 nm.

parvalbumin, which have relatively buried Trp residues, show almost no variation in r with wavelength (this is also the case for aldolase and fd phage). The decrease in r with increasing wavelength seen for some proteins may reflect (*a*) heterogeneity of the protein sample due, for example, to the existence of multiple conformations of the protein or to sample impurity, or (*b*) a wavelength dependence of the fluorescence lifetime of the Trp residues caused by dipolar relaxation processes occurring on the same time scale as the fluorescence decay (41).

On the other hand, the apparent emission wavelength independence of r for ribonuclease T_1 suggests that for the buried Trp residue in this protein, and possibly for buried residues in other proteins, that a minimum degree of dipolar relaxation occurs about the excited indole ring (consistent with the fine structured emission [42] and our observed emission wavelength independence of τ [20] for ribonuclease T_1).

The apparent ϕ values experimentally obtained for the series of single Trp proteins are in most cases approximately equal to ϕ_h, the calculated rotational correlation time for a hydrated sphere of corresponding molecular weight (compare the fifth and sixth columns in Table II). Thus for most proteins, the observed time constant for the depolariztion process appears to reflect the overall Brownian rotation of the protein. Both positive and negative deviations between the experimental ϕ and ϕ_h are seen, however, which may be a result of (*a*) experimental error, (*b*) the inadequacy of Eq. 3 to describe the global rotation of the protein (i.e., due to the fact that the protein is asymmetric or the hydration value of 0.3 cm^3/g is not appropriate), (*c*) the existence of a heterogeneous fluorescence lifetime of the protein (see Theory section), or (*d*) the contribution of internal segmental motion to the observed ϕ (see Theory section). For these reasons any agreement (or lack of agreement) between experimental and calculated rotational correlation times should be interpreted with caution. Note also that the fluorescence lifetime values needed to calculate ϕ(app) were obtained from various sources (see footnotes in Table II), and this introduces some uncertainty.

For myelin basic protein, we find the greatest disparity betwen the observed and calculated ϕ values, with the observed ϕ being <50% of the value of ϕ_h. This sizable discrepancy strongly suggests a contribution to the observed ϕ from internal rotation of the Trp residue in this protein and is consistent with the anisotropy decay studies of Munro et al. (8) in which a very small rotational correlation time was found.

The magnitude of the apparent r_o values can provide additional insight concerning the existence of rapid segmental motion of the Trp residues in the set of proteins. The r_o values are found to range from 0.20 to 0.32. The value for the limiting anisotropy of indole or tryptophan in frozen solvents is found by most workers to be in the range

of 0.30–0.31 (with 300 nm as the excitation wavelength [38, 39, 43]). For *N*-acetyl-L-tryptophanamide in glycerol, we find an r_o of 0.290 on extrapolation of r measurements from room temperature to $T/n \rightarrow 0$ (lowest temperature, 2°C). We have also measured the anisotropy of two very large protein aggregates, aldolase (160,000 MW) and fd bacteriophage 16 × 10^6 MW) and find apparent r_o values of 0.303 and 0.311, respectively, on extrapolation to $T/\eta \rightarrow 0$. The largest r_o(app) value obtained in our QREA studies was 0.32. Thus, we find an r_o value of 0.31 ± 0.02 at an excitation wavelength of 300 nm to be an appropriate limiting value for comparison in our studies.

For ribonuclease T_1 the r_o(app) of ~0.32 indicates an absence of internal motion of the Trp residue in this protein. For other proteins, the r_o(app) are smaller, indicating that rapid segmental motion of the Trp residues takes place. We are unable to describe precisely the time scale of this rapid motion; we can only suggest that the time constant for such motion is subnanosecond. A qualitative description of this motional freedom can be given in terms of an angle, θ, corresponding to a cone over which this motion takes place (see Eq. 5). The values of θ for the various proteins are given in Table II. The θ values are seen to range from 0° to 30°.

The information we have obtained in these QREA experiments is consistent with other information concerning the location of Trp residues in the various proteins. For example, our data for ribonuclease T_1 are consistent with the Trp in this protein being rigidly buried (43, 44). Likewise the ϕ(app) and r_o(app) for cod parvalbumin indicate that its Trp residue is relatively restricted, which is consistent with other fluorescence data showing this residue to be buried (45) (also note the low k_q for acrylamide quenching in Table II). For ACTH, glucagon, melittin monomer, and myelin basic protein, on the other hand, the Trp residues appear to be quite flexible, as expected for these solvent-exposed residues.

Some of our ϕ(app) values can be compared with literature values obtained from anisotropy decay experiments as follows: for nuclease, 8.6 ns (7) and 9.7 ns (at 20°C [8]), as compared with our value of 9.1 ns; for HSA at 8°C, 31 ns (8), as compared with our value of 39 ns; for monomeric and tetrameric melittin, 1.1 and 3.7 ns (46), respectively, as compared with our values of 1.5 and 2.5 ns. These comparisons show that the QREA method can provide rotational correlation time data that are comparable with those obtained using the more technically demanding anisotropy decay method.

Use of QREA to Study Changes in Protein Conformation

Steady state fluorescence anisotropy measurements have been widely used to investigate protein-protein aggregation phenomena and protein unfolding reactions, the basis for this application being that the emission anisotropy of a fluorescent reporter group will generally tend to be higher for the more aggregated or structured conformations of the macromolecule. As we will demonstrate by examples below, the QREA method can also be readily applied to study protein aggregation/unfolding reactions and can provide additional information concerning such reactions in terms of the ϕ(app) and r_o(app) values.

In Fig. 5, studies of four different protein systems undergoing a conformational change are shown. Two of these are the monomer ⟺ dimer equilibrium of β-lactoglobulin (47) and the monomer ⟺ tetramer equilibrium of melittin (48). For both of these cases we find a significant increase in ϕ(app) for the more aggregated form (see Table II). In the case of β-lactoglobulin the increase in ϕ(app) correlates very well with the increase in the size of the protein in going from the monomer to the dimer. For melittin the correlation between ϕ(app) and protein size is not as good, which suggests that internal mobility of the Trp side chain may contribute to the ϕ(app) values.

The pH-induced N ⟺ F transition of HSA (49) is another type of protein conformational change that can be studied by QREA experiments. As the pH of an HSA solution is lowered below pH 4, the various lobes of the protein are believed to separate from one another. We find, as illustrated in Fig. 5 *C*, that the ϕ(app) of the low pH form of HSA is significantly smaller than that of the neutral pH form. Whereas the ϕ(app) at neutral pH is consistent with the global rotation of a spherical protein of 69,000 MW, the ϕ(app) value at low pH corresponds to the segmental motion of a 30,000 MW lobe of HSA. Our results are thus quite in line with the molecular view of the N ⟺ F transition of HSA.

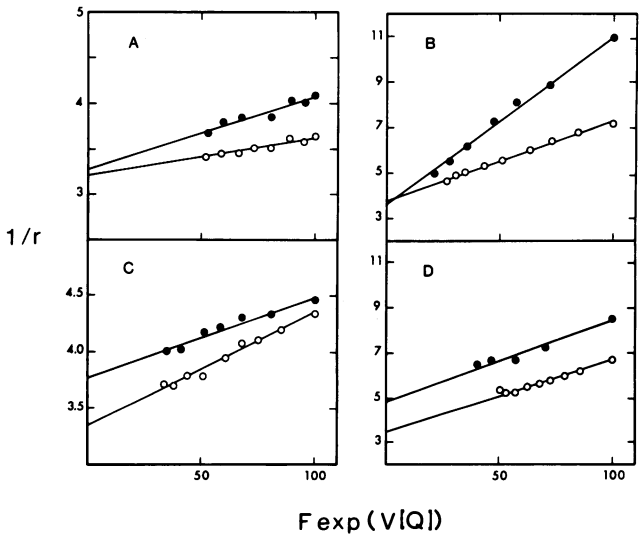

FIGURE 5 QREA studies of protein conformational changes. (*A*) β-lactoglobin monomer (•) and dimer (○). (*B*) melittin monomer (•) and tetramer (○). (*C*) HSA *N* form (•) and *F* form (○). (*D*) Parvalbumin holoprotein (•) and Ca^{+2} deficient apoprotein (○). Conditions are given in Table II.

A fourth example of a protein conformation change that we have investigated involves the effect of bound Ca^{+2} on the structure of cod parvalbumin. With two moles of Ca^{+2} bound per mole of this protein, the fluorescence of its single Trp residue is very blue (λ_{max} = 320 nm [34, 45]). On the removal of Ca^{+2}, a dramatic red shift of 25 nm occurs, suggesting that the Trp residue becomes more exposed to solvent (45). The steady state anisotropy of parvalbumin decreases from 0.15 to 0.12 upon removal of Ca^{+2}. From a QREA study with acrylamide as quencher we find the drop in anisotropy to be due almost entirely to a decrease in r_o(app) upon Ca^{+2} removal; the ϕ(app) appears to be approximately the same for the two states of the protein (actually slightly larger for the apoprotein). This suggests that loss of the metal ions leads to a significant increase in the internal mobility of the Trp residue (for which $\theta = 28°$ for the apoprotein, as compared to 12° for the holoprotein). For both states of the protein the apparent rotational correlation time reflects the global rotation of the protein, indicating that the shape of the protein is not greatly changed by the removal of Ca^{+2}.

Studies with Multitryptophan-containing Proteins

The QREA studies presented thus far have focused primarily on single-Trp–containing proteins and the information [ϕ(app) and r_o(app)] that can be obtained to describe the depolarization processes for such Trp residues. In this section, we consider the use of this method to study multi-Trp proteins, with emphasis on the strategy of employing a selective quencher for such studies.

LADH is a dimeric protein that is particularly amenable to this type of study. Due to its symmetry, LADH has only two types of Trp residues, Trp 15 and Trp 314. The microenvironment of these two residues is markedly different, which results in the fluorescence of LADH being quite heterogeneous (9, 20, 23, 24). The fluorescence lifetime of Trp 15 and Trp 314 have been determined to be ~7 ns and 3.5 ns, respectfully, by both fluorescence decay (9) and phase/modulation studies (20). Trp 314, whose fluorescence is relatively blue and fine structured, is found to be almost completely inacessible to the polar quenchers acrylamide (24) and iodide (23). Trp 15, on the other hand, is exposed to solvent and can be readily quenched by either acrylamide or iodide.

The ability of Trp 15 to be selectively quenched makes it possible to determine the anisotropy of each residue by measurement of r as a function of [Q]. In Fig. 6 a plot of $1/r$ vs. fluorescence intensity and a direct plot of r vs. fluorescence intensity for studies with acrylamide as quencher are shown. (Compare with Fig. 2 and see paragraph *c* in Theory section Multitryptophan-containing Proteins.) One cannot determine r_o(app) and ϕ(app) values from the plot in Fig. 6 *A*, due to the fact that selective quenching is occurring in this system. From the anisotropy

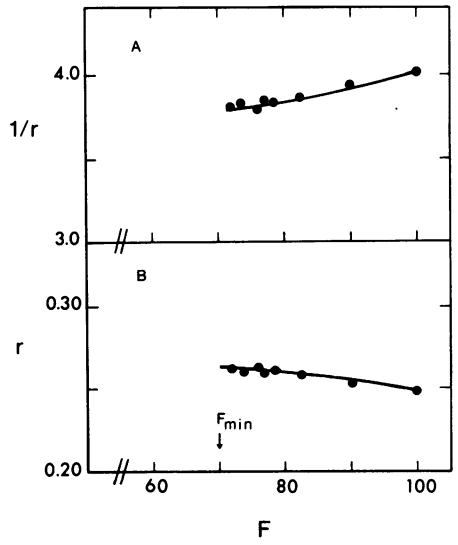

FIGURE 6 QREA studies with LADH using acrylamide as quencher. (*A*) Perrin plot. (*B*) Plot of r vs. F. Emission monitored at 340 nm. From a plot of $F_o/\Delta F$ vs. $1/[Q]$ (not shown), F_1 (= F_{15}) was determined to be 0.30 at λ_{ex} = 300 nm and λ_{em} = 340 nm. This value was used to calculate r_1 (=r_{15}) and r_2 (=r_{314}) values given in Table II.

values at [Q] = 0 and [Q] = ∞ (i.e., the r value at F_{min}) in Fig. 6 *B*, one can dissect the values of r_{15} and r_{314}. To do this, values of f_{15} and f_{314} must be obtained from an analysis of the quenching data (22, 24, see legend of Fig. 6). The resultant values for r_{15} and r_{314} are given in Table II. The value for r_{314} is rather large. This is reasonable since Trp 314 is deeply buried at the subunit interface of this protein. If one assumes that the r_o value for Trp 314 is 0.31 (i.e., there is essentially no internal motion for this residue), a ϕ_{314} value of 25 ns is calculated. This value is approximately equal to the value of 30 ns that one would expect for the rotation of an 80,000 MW protein. Thus, our data are consistent with Trp 314 being buried in a very inflexible domain of the protein.

The r_{15} value, in contrast, is much lower and indicates that this surface residue enjoys a much greater degree of motional freedom. It is unclear, however, if the lower r value for Trp 15 can be ascribed to very rapid internal motion [i.e., a reduced r_o(app)], or if the r_o(app) is approximately the same but the ϕ(app) value for Trp 15 is low (i.e., as would be the case if the time constant for internal motion was of the same order of magnitude as that for global rotation of the protein). For the former interpretation, an r_{15} of 0.21 would correspond to an r_o(app) of 0.25. This in turn, would correspond to very rapid motion of Trp 15 within a cone of angle 20°, with the remaining anisotropy decaying with a rotational correlation time corresponding to that for global rotation of the protein (i.e., ϕ = 30 ns). Alternatively, one can consider the depolarization of Trp 15 to be described by a rotational correlation time of 11 ns [with r_o(app) assumed to remain at 0.31]. This correlation time is less than one-half of that for the

rotation of the protein. With either description, Trp 15 is characterized as having a significant degree of segmental freedom of motion. The first interpretation given above (very rapid motion within an angle of 20°) is probably the most realistic one, in view of our above studies with single-Trp proteins which show that ϕ(app) is usually (except for myelin basic protein) within 30% of the calculated ϕ_h value. If this is the case, our determined r_{15} and r_{314} values are consistent with the anisotropy decay studies with LADH by Ross et al. (9). These workers found the anisotropy decay of this protein to be a single exponential with a rotational correlation time of 36 ns (at 27.5°C).

Lysozyme is another multi-Trp protein whose fluorescence is known to be very heterogeneous (50, 51). Tryptophan residues 62 and 108 of lysozyme are believed to be the primary emitters of this protein (50), with Trp 62 being the most exposed to solvent (and presumably the most accessible to collisional quenchers [22]). As in the above studies with LADH, we have been able to resolve the anisotropy of the buried and surface Trp residues by using selective quenchers. With iodide as quencher, we obtain r values of 0.16 and 0.22 for the accessible and inaccessible residues, respectively. Similar experiments with acrylamide yield r values of 0.17 and 0.26 for the accessible and inaccessible residues. The slight difference in the corresponding r values with the two quenchers undoubtedly arises from the fact that more (or different) Trp residues are accessible to acrylamide, as compared with iodide. In both cases, however, the buried residues are found to have the higher anisotropy. This may reflect the restricted mobility of such residues, but may also be due to the fact that the buried residues have a lower fluorescence lifetime than the surface residues (51).

CONCLUDING REMARKS

We have presented a survey study demonstrating the application of the QREA method to characterize the dynamics of the fluorescence depolarization of Trp residues in proteins. The experimental method is technically simple, but rich in the amount of information that it can provide. The apparent rotational correlation times obtained by this method are generally consistent with those expected for global Brownian rotation of the proteins and are in good agreement with similar data obtained by more elaborate anisotropy decay studies. The apparent limiting anisotropy values obtained for some proteins suggest that rapid internal rotation of Trp residues occurs over an angle of up to 30°. In addition to the apparent ϕ and r_o values obtained in QREA studies, it should be recalled that information of the solvent exposure of Trp residues is also provided in these experiments in terms of the magnitude of the quenching rate constant (21).

The results provided by these studies on the mobility of Trp residues (or lack of independent mobility in some cases) in proteins support other recent magnetic resonance studies (52, 53) and theoretical calculations (54, 55) concerning the dynamics of amino acid side chains in proteins. In particular, it is interesting to note that the molecular-dynamics calculations of McGammon and co-workers (55) predict that rapid torsional motion of aromatic side chains over an angle of 30° may easily occur in proteins.

For proteins containing more than one fluorescing Trp residue, the QREA technique can be used to determine the anisotropy of individual residues if selective quenching of the different residues can be achieved. The latter possibility offers an advantage, in some instances, over anisotropy decay studies. As our work with LADH illustrates, anisotropy decay studies might yield the same rotational correlation time for two classes of fluorophores on a protein. A selective quenching QREA study, on the other hand, might be able to reveal the existence of rapid segmental motion of one or both of the fluorophores.

The QREA method also offers some advantages over steady state anisotropy studies in which either temperature or bulk viscosity is varied. A problem with obtaining a Perrin plot by varying temperature is the possibility of having a temperature-induced conformational change or having thermally activated internal depolarizing motions (12, 13, 15). QREA studies can be performed at a series of fixed temperatures, thus allowing such temperature effects to be investigated. Perrin plots obtained by varying viscosity can be experimentally tedious. The matter of the viscosity dependence of the fluorescence lifetime must be dealt with, and the amount of co-solute (i.e., glycerol or sucrose) that is usually added can amount to up to 50% by weight. By comparison, the amount of acrylamide added in QREA experiments is usually <4% by weight. Because the relative position of the L_a band of indole is environment dependent (56), complications are expected to be fewer in the quenching QREA experiments.

The quencher used for such studies does not have to be a unity-efficient quencher, but should quench primarily by a collisional process. (For selective quenching studies with a multi-Trp protein, the quenching process does not have to be collisional, so long as one type of residue can be selectively quenched.)

The quenchers that have been used most successfully thus far with proteins and that are the most likely choices for QREA studies are oxygen, iodide, and acrylamide (19, 21, 22). The charged quencher iodide is probably the most selective of these quenchers and thus should be useful in dissecting the anisotropy of classes of residues in multi-Trp proteins. However, iodide is unable to quench the fluorescence of certain proteins (e.g., ribonuclease T_1, parvalbumin, β-lactoglobulin), which makes QREA experiments impossible in these cases. Oxygen, a much smaller quenching probe, is able to readily penetrate the structure of proteins and thus is less useful for selective quenching/anisotropy studies. Because the rate constants for oxygen quenching fall within a rather narrow range of $1–5 \times 10^9$ M^{-1} (19, 20) one can assume to the first approximation, a single rate constant for the oxygen

quenching of a multi-Trp protein. This assumption allows an estimation of a rotational correlation time for multi-Trp proteins to be made from oxygen-quenching QREA studies (17). Complications due to heterogeneity in the fluorescence lifetime and degree of segmental motion of the different Trp residues may still need to be considered in these cases.

Acrylamide combines the favorable advantage of each of the above quenchers for QREA studies. Acrylamide is able to quench the fluorescence of most of the Trp residues in proteins, but, due to the large range in quenching rate constants ($<0.05 - 4 \times 10^9$ M^{-1} s^{-1}) for individual residues, selective quenching of multi-Trp proteins is possible (21). As demonstrated with lysozyme and LADH, this enables one to evaluate the anisotropy of the quenched and unquenched classes of Trp residues.

Finally, we wish to point out that although the present QREA studies have focused on the intrinsic fluorescence of tryptophanyl residues in proteins, that similar studies could be performed using attached extrinsic probes. In particular, the strategic use of extrinsic probes with long τ_0 would enable the determination of rotational correlation times for macromolecular structures larger than those studied here.

We are grateful to Dr. F. Walz, Kent State University, and Dr. R. Webster, Duke University, for generously providing protein samples. We also express appreciation to Dr. C. A. Ghiron, University of Missouri, and Dr. J. W. Longworth, Oak Ridge National Laboratories, for helpful discussions, and to Dr. D. Jameson, University of Pennsylvania, Dr. R. Hall, University of Illinois, and Tom Markell, University of Virginia, for providing assistance in making fluorescence lifetime measurements.

This work was supported by National Science Foundation grant PCM-8206073.

Recieved for publication 14 December 1982 and 7 April 1983.

REFERENCES

1. Wahl, P. 1975. Decay of fluorescence anisotropy. Biochemical Fluorescence: Concepts. R. F. Chen and H. Edelhoch, editors. Marcel Dekker, Inc., New York, 1:1–41.
2. Yguerabide, J., H. F. Epstein, and L. Stryer. 1970. Segmental flexibility in an antibody molecule. *J. Mol. Biol.* 51:573–590.
3. Lovejoy, C., D. A. Holowka, and R. E. Cathou. 1977. Nanosecond fluorescence spectroscopy of pyrenebutyrate-anti-pyrene antibody complexes. *Biochemistry.* 16:3668–3672.
4. Hanson, D. C., J. Yguerabide, and V. N. Schumaker. 1981. Segmental flexibility of immunoglobulin G antibody molecules in solutions: a new interpretation. *Biochemistry.* 20:6842–6852.
5. Mendelsohn, R. A., M. F. Morales, and J. Botts. 1973. Segmental flexibility of the S-1 moiety of myosin. *Biochemistry.* 12:2250–2255.
6. Harvey, S. C., and H. C. Cheung. 1977. Fluorescence depolarization studies on the flexibility of myosin rod. *Biochemistry.* 16:5181–5187.
7. Brochon, J. C., P. Wahl, and J. C. Auchet. 1974. Fluorescence time-resolved spectroscopy and fluorescence anisotropy decay of *Staphylococcus aureus* endonuclease. *Eur. J. Biochem.* 41:577–583.
8. Munro, I., I. Pecht, and L. Stryer. 1979. Subnanosecond motions of tryptophan residues in proteins. *Proc. Natl. Acad. Sci. USA.* 76:56–60.
9. Ross, J. B. A., C. J. Schmidt, and L. Brand. 1981. Time-resolved fluorescence of the two tryptophans in horse liver alcohol dehydrogenase. *Biochemistry.* 20:4369–4377.
10. Weber, G. 1952. Polarization of the fluorescence of macromolecules. Theory and experimental method. *Biochem. J.* 51:145–155.
11. Weer, G. 1952. Polarization of the fluorescence of macromolecules. Fluorescent conjugates of ovalbumin and bovine serum albumin. *Biochem. J.* 51:155–167.
12. Wahl, P., and G. Weber. 1967. Fluorescence depolarization of rabbit gamma globulin conjugates. *J. Mol. Biol.* 30:371–382.
13. Weltman, J. K., and G. M. Edelman. 1965. Fluorescence polarization of human αG-immunoglobulins. *Biochemistry.* 6:1437–1447.
14. Semisotnov, G. V., K. Kh. Zikherman, S. B. Kasatkin, O. B. Ptitsyn, and E. V. Anufrieva. 1981. Polarized luminescence and mobility of tryptophen residues in polypeptide chains. *Biopolymers.* 20:2287–2309.
15. Brochon, J. C., P. Wahl, and J. C. Auchet. 1972. Measurement of the fluorescence anisotropy decay of γ-globulin and its Fab, Fc, and $F(ab)_2$ fragments labeled with 1-sulfonyl-5-dimethylaminonaphthalene. *Eur. J. Biochem.* 25:20–32.
16. Teale, F. W. J., and R. A. Badley. 1970. Polarization of the intrinsic and extrinsic fluorescence of pepsinogen and pepsin. *Biochem. J.* 116:341–348.
17. Lakowicz, J. R., and G. Weber. 1981. Nanosecond segmental mobilities of tryptophan residues in proteins observed by lifetime-resolved fluorescence anisotropies. *Biophys. J.* 32:591–600.
18. Lakowicz, J. R., B. Maliwal, H. Cherek, and A. Balter. 1982. Rotational freedom of tryptophan residues in proteins and peptides. *Biochemistry* 22:1741–1752.
19. Lakowicz, J. R., and G. Weber. 1973. Quenching of protein fluorescence by oxygen. Detection of structural fluctuations in proteins on the nanosecond time scale. *Biochemistry.* 12:4171–4179.
20. Eftink, M. R., and D. M. Jameson. 1982. Acrylamide and oxygen fluorescence quenching studies with liver alcohol dehydrogenase using steady-state and phase fluorometry. *Biochemistry.* 21:4443–4449.
21. Eftink, M. R., and C. A. Ghiron. 1976. Exposure of tryptophan residues in proteins. Quantitative determination by fluorescence quenching studies. *Biochemistry.* 15:672–680.
22. Lehrer, S. S. 1971. Solute perturbation of protein fluorescence. The quenching of the tryptophyl fluorescence of model compounds, and of lysozyme by iodide ion. *Biochemistry.* 10:3254–3263.
23. Abdallah, M. A., J. F. Biellman, P. Wiget, R. Joppich-Kuhn, and P. L. Lusi. 1978. Fluorescence quenching and energy transfer in complexes between horse-liver alcohol dehydrogenase and coenzymes. *Eur. J. Biochem.* 89:397–405.
24. Eftink, M. R., and L. A. Selvidge. 1982. Fluorescence quenching of liver alcohol dehydrogenase by acrylamide. *Biochemistry.* 21:117–125.
25. Kuntz, I. D., Jr., and W. Kauzmann. 1974. Hydration of proteins and polypeptides. *Adv. Protein. Chem.* 28:239–345.
26. Belford, G. G., R. L. Belford, and G. Weber. 1972. Dynamics of fluorescence polarization in macromolecules. *Proc. Natl. Acad. Sci. USA.* 69:1392–1393.
27. Small, E. W., and I. Isenberg. 1977. Hydrodynamic properties of a rigid molecule: rotational and linear diffusion and fluorescence anisotropy. *Biopolymers.* 16:1907–1928.
28. Gottlieb, Y. Y., and P. Wahl. 1963. Theory of the polarization of fluorescence of macromolecules with a mobile emitter group around a rotation axis. *J. Chim. Phys. Physicochim. Biol.* 60:849–856.
29. Lipari, G., and A. Szabo. 1980. Effect of librational motion on fluorescence depolarization and nuclear magnetic resonance

relaxation of macromolecules and membranes. *Biophys. J.* 30:489–506.

30. Grinvald, A., and I. Z. Steinberg. 1976. The fluorescence decay of tryptophan residues in active and denatured proteins. *Biochim. Biophys. Acta.* 427:663–678.
31. Szabo, A. G., and D. M. Rayner. 1980. Fluorescence decay to tryptophan conformers in aqueous solution. *J. Am. Chem. Soc.* 102:554–563.
32. Eftink, M. R., and C. A. Ghiron. 1981. Fluorescence quenching studies with proteins. *Anal. Biochem.* 114:199–227.
33. Chen, R. F. 1967. Removal of fatty acids from serum albumin by charcoal treatment. *J. Biol. Chem.* 242:172–181.
34. Horrocks, W. A., and W. E. Collier. 1981. Lanthanide ion luminescence probes. Measurement of distance between intrinisic protein fluorophores and bound metal ions: quantitation of energy transfer between tryptophan and terbium (III) or europium (III) in the calcium binding protein parvalbumin. *J. Am. Chem. Soc.* 103:2856–2862.
35. Blum, H. E., P. Lehky, L. Kohler, E. A. Stein, and E. Fischer. 1977. Comparative properties of vertebrate parvalbumins. *J. Biol. Chem.* 252:2834–2838.
36. Shinitzky, M., A. C. Dianoux, C. Gitler, and G. Weber. 1971. Microviscosity and order in the hydrocarbon region of micelles and membranes determined with fluorescent probes. I. Synthetic micelles. *Biochemistry.* 10:2106–2113.
37. Teale, F. W. J. 1969. Fluorescence depolarization by light-scattering scattering in turbid solutions. *Photochem. Photobiol.* 10:363–374.
38. Weber, G. 1960. Fluorescence-polarization spectrum and electronic-energy transfer in tyrosine, tryptophan and related compounds. *Biochem. J.* 75:335–345.
39. Valeur, B., and G. Weber. 1977. Resolution of the fluorescence excitation spectrum of indole into ^1L_a and ^1L_b excitation bonds. *Photochem. Photobiol.* 25:441–444.
40. Weber, G., and M. Shinitzky. 1970. Failure of energy transfer between identical aromatic molecules on excitation at the long edge of the absorption spectrum. *Proc. Natl. Acad. Sci. USA.* 65:823–830.
41. Lakowicz, J. R., and H. Cherek. 1980. Dipolar relaxation in proteins on the nanosecond timescale observed by wavelength-resolved phase fluorometry of tryptophan fluorescence. *J. Biol. Chem.* 255:831–834.
42. Longworth, J. W. 1968. Excited state interactions in macromolecules. *Photochem. Photobiol.* 7:587–596.
43. Ghiron, C. A., and J. W. Longworth. 1979. Transfer of singlet energy within trypsin. *Biochemistry.* 18:3828–3832.
44. Eftink, M. R., and C. A. Ghiron. 1977. Exposure of tryptophanyl residues and protein dynamics. *Biochemistry.* 16:5546–5551.
45. Permyakov, E. A., V. V. Yarmolemko, V. I. Emelyanenko, E. A. Burstein, J. Closset, and C. Gerday. 1980. Fluorescence studies of the calcium binding to Whiting parvalbumin. *Eur. J. Biochem.* 109:307–315.
46. Georghiou, S., M. Thompson, and A. K. Mukhopadhyay. 1981. Melittin-phospholipid interaction evidence for melittin aggregation. *Biochim. Biophys. Acta.* 642:429–432.
47. Townsend, R., T. T. Herskovits, S. M. Timasheff, and M. J. Gorbunoff. 1969. The state of amino acid residues in β-lactoglobulin. *Arch. Biochem. Biophys.* 129:567–580.
48. Talbot, J. C., J. Dufourcq, J. deBony, J. F. Faucon, and C. Lussan. 1979. Conformatinal change and self-association of monomeric melittin. *FEBS (Fed. Eur. Biochem. Soc.) Lett.* 102:191–193.
49. Foster, J. F. 1960. The Plasma Proteins. Putman, F. W., editor. Academic Press, Inc., New York. 179–239.
50. Imoto, T., L. S. Forster, J. A. Rupley, and F. Tanaka. 1971. Fluorescence of lysozyme: emissions from tryptophan residues 62 and 108 and energy migration. *Proc. Natl. Acad. Sci. USA.* 69:1151–1155.
51. Formoso, C., and L. S. Forster. 1975. Tryptophan fluorescence lifetime in lysozyme. *J. Biol. Chem.* 250:3738–3745.
52. Hull, W. E., and B. D. Sykes. 1975. Fluorotyrosine alkaline phosphatase: internal mobility of individual tyrosines and the role of chemical shift anisotropy as a ^{19}F nuclear spin relaxation mechanism of proteins. *J. Mol. Biol.* 98:121–153.
53. Ribeiro, A. A., R. King, C. Resstivo, and O. Jardetzky. 1980. An approach to the mapping of internal motions in proteins. Analysis of ^{13}C NMR relaxation in the bovine pancreatic trypsin inhibitor. *J. Am. Chem. Soc.* 102:4040–4051.
54. Gelin, B. R., and M. Karplus. 1975. Sidechain torsional potentials and motion of amino acids in proteins: bovine pancreatic inhibitor. *Proc. Natl. Acad. Sci. USA.* 72:2002–2006.
55. McGammon, J. A., P. G. Wolynes, and M. Karplus. 1979. Picosecond dynamics of tyrosine side chains in proteins. *Biochemistry.* 18:927–942.
56. Andrews, L. J., and L. S. Forster. 1972. Protein difference spectra. Effect of solvent and charge on tryptophan. *Biochemistry.* 11:1875–1879.
57. Spencer, R. D., and G. Weber. 1969. Measurements of subnanosecond fluorescence lifetimes with a cross-correlation phase fluorometer. *Ann. NY Acad. Sci.* 158:361–376.